Structural Stability of the Square Flux Line Lattice in YNI_2B_2C and $LuNi_2B_2C$ Studied with Small Angle Neutron Scattering

M. R. Eskildsen,[1] P. L. Gammel,[2] B. P. Barber,[2] A. P. Ramirez,[2] D. J. Bishop,[2] N. H. Andersen,[1] K. Mortensen,[1] C. A. Bolle,[3] C. M. Lieber,[3] and P. C. Canfield[4]
[1]*Risø National Laboratory, DK-4000 Roskilde, Denmark*
[2]*Bell Laboratories, Lucent Technologies, Murray Hill, New Jersey 07974*
[3]*Harvard University, Cambridge, Massachusetts 02138*
[4]*Iowa State University, Ames, Iowa 50011*
(Received 24 February 1997)

We have studied the flux line lattice in YNi_2B_2C and $LuNi_2B_2C$, the nonmagnetic end members of the borocarbide superconductors using small angle neutron scattering and transport. For fields, $\mathbf{H} \parallel \mathbf{c}$, we find a square symmetric lattice which disorders rapidly above $H/H_{c2} \sim 0.2$, well below the "peak effect" at $H/H_{c2} = 0.9$. The results for $H/H_{c2} < 0.2$ can be understood within the collective pinning model, and are controlled by the tilt modulus c_{44}. For $H/H_{c2} > 0.2$, the disordering appears to be associated with the field dependence of the shear modulus, c_{66}. [S0031-9007(97)03634-X]

PACS numbers: 74.60.Ge

The borocarbide intermetallic superconductors have shown a wide range of unusual and interesting properties. These compounds, with chemical formula $(R)Ni_2B_2C$ assume the filled $ThCr_2Si_2$ structure, ubiquitous to ternary intermetallics [1]. For $R =$ Y, Dy, Ho, Er, Tm, or Lu the materials are strongly type-II superconductors ($\kappa \sim 5$–15) with T_c up to 16 K and H_{c2} which can exceed 10 T [2–6]. Several members of this class show magnetic transitions which persist in the superconducting phase, reviving interest in the detailed coexistence of superconductivity and magnetism [7,8]. The structure and dynamics of the flux line lattice (FLL) in these materials are also remarkable. At high fields, a square FLL is seen, as opposed to the hexagonal structure generic to high κ materials [9,10]. This undergoes a field induced square to hexagonal transition at low field, driven by a coupling to the anisotropic Fermi surface [11]. This symmetry transition, and the associated changes in the FLL elastic moduli, were shown to influence the microwave transport data. Further, the FLL has been found to couple to magnetic order in $ErNi_2B_2C$ (Er:1221), as evidenced by a rotation and disordering of the FLL in the metamagnetic superconducting phase below 2.3 K [9].

In this Letter we report on studies of YNi_2BC2 (Y:1221) and $LuNi_2B_2C$ (Lu:1221), the two nonmagnetic end members of this series, using both small angle neutron scattering (SANS) and dc transport measurements. Our data allow two important conclusions to be reached. First, both materials have a low field hexagonal FLL which transforms into a square FLL in the 1 kOe range, in agreement with recent calculations based on nonlocal corrections to the London model [12]. Second, we find that the FLL has a maximum in its longitudinal correlation length near $H/H_{c2} \sim 0.2$. Below this field, the SANS data can be understood within the traditional collective pinning model using the measured critical currents and the FLL tilt modulus [13]. Above this field, the longitudinal correlation lengths are dramatically reduced below this estimate.

We can fit our high field data for $\mathbf{H} \parallel \mathbf{c}$ and at an angle from the c axis using the field dependence of the shear modulus c_{66}. This is in disagreement with the weak collective pinning model, in which the longitudinal correlations are determined by the tilt modulus. The shear modulus has a peak at $H/H_{c2} \sim 0.3$, after which it decreases, ultimately leading to the peak effect in the transport critical current when the FLL is completely amorphous at $H/H_{c2} \sim 0.9$. Our data then represent direct measurements of the gradual disordering of the FLL in high κ materials. Previous studies in low κ, marginally type-II niobium showed a disordering in the transverse FLL correlations, in agreement with the simple weak collective pinning model [14]. Understanding the shear properties plays a central role in the dynamics of the FLL, particularly the phase transitions, such as FLL melting seen in both the high temperature and borocarbide [15] superconductors. Measurements of c_{66} have mostly been inferred from its dynamical consequences [16], leaving static data as an important point of comparison.

The single crystal materials used in these experiments were flux grown platelets with the c axis perpendicular to the flat surface [5]. Isotopically enriched B^{11} was used to increase thermal neutron penetration. Y:1221 has a superconducting transition temperature $T_c = 15.6$ K, and Lu:1221 has $T_c = 16.6$ K [3]. Sample dimensions were typically $8 \times 8 \times 1$ mm^3 with masses of 200–400 mg. For transport studies, $3 \times 1 \times 0.3$ mm^3 bars were cut from the large crystals, and etched in HF and aqua regia to reduce surface pinning.

The SANS experiments were performed in the cold neutron guide hall of the Risø National Laboratory DR3 reactor. Neutrons with wavelengths λ_n between 3.8 and

12.4 Å, energy spread $\Delta\lambda_n/\lambda_n = 0.18$, and angular divergence of $\sim 0.1°$ were used. The Bragg scattered neutrons were counted using an area detector located 6 m from the sample. Magnetic fields from 500 Oe to 35 kOe were applied parallel to the neutron beam. In most of the experiments, the c axis was parallel to the field, but we also performed experiments with the field rotated in the ac plane. In all cases a field cool to $T = 2.2$ K was performed.

The reflectivity of a single FLL Bragg peak allows detailed measurements of the penetration depth λ and coherence length ξ, the two microscopic length scales in the superconducting state. The reflectivity is given by $R = (2\pi\gamma^2\lambda_n^2 t/16\phi_0^2 q)H_1^2$, where $\gamma = 1.91$ is the gyromagnetic ratio of the neutron, t is the sample thickness, ϕ_0 is the flux quantum, and $q = 2\pi\sqrt{(B/\phi_0)}$ is the scattering vector of the first order square FLL Bragg reflection. First order Ginzburg-Landau corrections to the London model result in a magnetic form factor for the square FLL $H_1 = (\phi_0/4\pi^2\lambda^2)\exp(-2\pi^2 B\xi^2/\phi_0)$ [17]. In Fig. 1, the field dependence of H_1^2 is plotted. In this semilog plot, the data lie on a straight line with a zero field intercept determined by λ and a slope determined by ξ. We find $\lambda = 1060 \pm 30$ Å for both compounds and $\xi = 88 \pm 3$ Å for Y:1221 and $\xi = 82 \pm 2$ Å for Lu:1221, in good agreement with literature values [4], and transport measurements yielding $H_{c2} = 65$ kOe. The $\xi = 71$ Å inferred from transport is about 10% below our estimate from SANS, as we have typically found with this model for the form factor.

SANS experiments can also be used to determine the FLL correlation lengths [18]. In addition to the detailed data on the rocking curve widths described below, we measured the radial and azimuthal widths of the FLL Bragg reflections in the plane of the detector, which give the positional and orientational correlation lengths of the FLL, respectively. Above 2 kOe, these widths stayed constant within the experimental resolution for all materials, fields, and angles studied. For fields **H** ∥ **c** above 2 kOe, the FLL was square, rotated 45° with respect to the underlying crystal and field independent except for the rocking curve width and the trivial field dependence of the flux line density. For rotation of the field by 30° in the ac plane away from c in Y:1221, the FLL was found to be hexagonal and distorted by the effective mass anisotropy $m_c/m_a = 1.8$ inferred from H_{c2} measurements, up to the highest measured field of 20 kOe. This rotation corresponds to having the field roughly in the (105) reciprocal lattice direction.

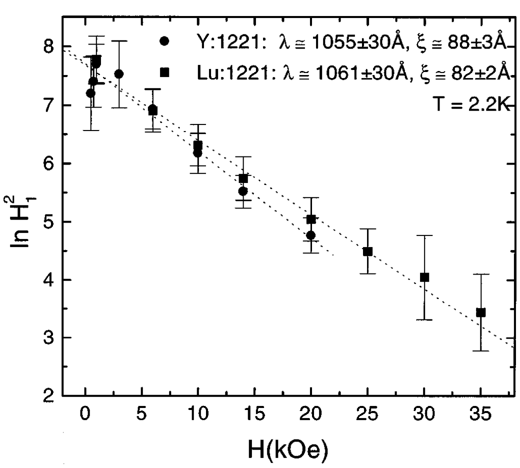

FIG. 1. Shown is the field dependence of the FLL magnetic form factor for Y:1221 and Lu:1221 at $T = 2.2$ K, from which $\xi(T)$ and $\lambda(T)$ are extracted.

In low field measurements performed on Y:1221 the azimuthal width of the FLL peaks were seen to broaden towards a ring of scattering below 1 kOe, similar to results in the magnetic compound Er:1221. In Er:1221, this is the onset of the square to hexagonal symmetry transition [11]. Our SANS data on Y:1221 show that both the high field square FLL and the square to hexagonal transition are generic to this class of materials independent of the presence of magnetism. The low field hexagonal lattice in Lu:1221 and Y:1221 was verified in decoration studies at 60 Oe and 4.2 K. Together, these data support recent calculations of FLL symmetry transitions based on nonlocal corrections to either the London model [12] or the Abrikosov model [10]. Corrections to the London model, which describe the low field, low temperature regime of the square-hexagonal transition, result from the anisotropy of the Fermi surface and produce a fourfold anisotropy. This anisotropy causes the FLL to undergo a second order phase transition from a low field, hexagonal lattice to a high field square lattice in clean systems, and provides quantitative comparison to our results in Er:1221. Magnetism does not appear to enter into the stability of the FLL, except insofar as it modifies certain fourth order Fermi surface averages. Additionally, the square to hexagonal transition field should increase as the field is rotated in the ac plane away from the c axis. Since our data at 30° tilt show a hexagonal FLL, the angle driven symmetry transformation is in qualitative agreement with this model.

In the remainder of this paper, we focus on the stable, high field FLL and how it disorders to accommodate the pinning force introduced by random disorder. Shown in the inset to Fig. 2 as a function of field, are the widths σ_m(FWHM), obtained by Lorentzian fits to the rocking curves and corrected for instrumental resolution [18]. The rocking curve width in this geometry measures how well correlated the flux lines are along their length, parallel to the applied field. In Fig. 2, the longitudinal correlation lengths are shown, determined from the rocking curves using $\xi_L/a_0 = (\pi\sigma_m)^{-1}$. Here $a_0 = 2\pi/q_0 = \sqrt{(\phi_0/B)}$ is the lattice parameter for the square FLL. For both materials and orientations, ξ_L/a_0 shows a similar behavior, increasing at low fields to a broad maximum near 10 kOe, and then gradually decreasing. It is important to emphasize that this maximum is not directly associated with either the square to hexagonal transition below 1 kOe or the

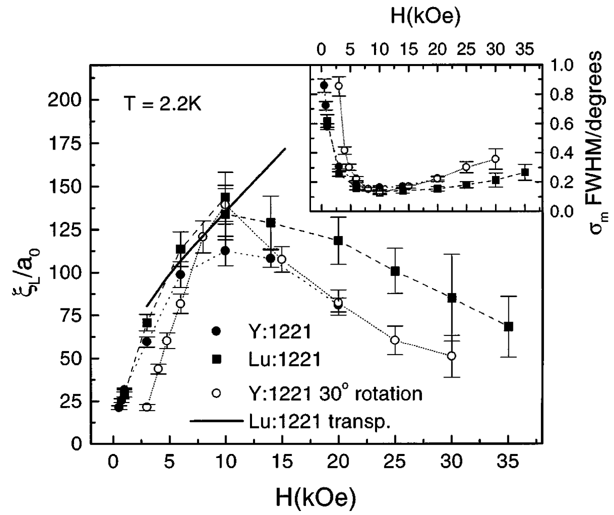

FIG. 2. The longitudinal FLL correlation lengths at $T = 2.2$ K are shown, extracted from the rocking curve widths via $\xi_L/a_0 = (\pi\sigma_m)^{-1}$. For $H \parallel c$, the Lu:1221 data are shown as the solid squares and the Y:1221 data are shown as the solid circles. Data on Y:1221 with the field rotated 30° in the ac plane are shown as the open circles. The longitudinal correlation length extracted from transport data using the collective pinning model for Lu:1221 and $H \parallel c$ are shown as the solid line, which agrees with the low field data. In the inset the raw rocking curve widths are shown.

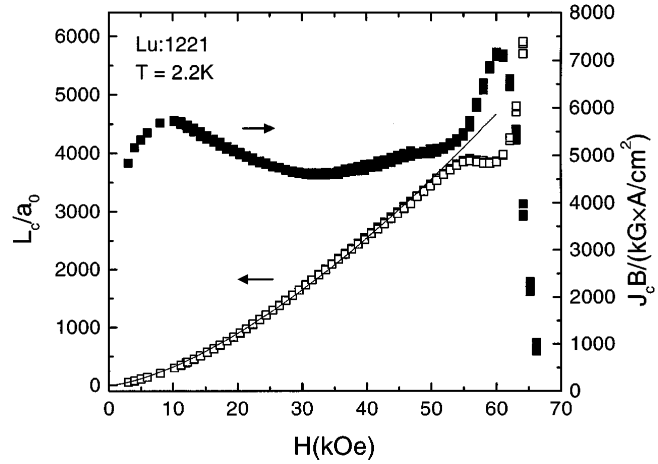

FIG. 3. Shown are the transport data for the pinning force density versus field at $T = 2.2$ K for Lu:1221 (solid squares) with $H \parallel c$. The relative longitudinal Larkin-Ovchinnikov length (open squares) extracted using simplest form of the collective pinning model is also shown. The line is a fit to $B^{3/2}$, the result for a constant pinning force.

pronounced "peak effect" at $H/H_{c2} \sim 0.9$ ($H = 60$ kOe) shown in Fig. 3. The maximum at 10 kOe is a quite unexpected behavior. In all previously studied high κ materials, and within the theoretical collective pinning framework, the longitudinal correlation length increases monotonically with field up to the peak effect. This general trend is understood as arising from vortex-vortex interactions which increasingly order the lattice with field. In particular, SANS studies of Nb show a longitudinal correlation length which increases monotonically, reaching a maximum at the peak effect, where the positional correlation length R_c has dropped to $\sim 1a_0$ [19]. In the case of the borocarbides, the low field estimate $R_c = (a_0/\lambda)\xi_L$ [20] yields positional correlations $\sim 50a_0$ throughout the regime of the 10 kOe maximum, far removed from the amorphous limit. Decoration studies show positional correlation lengths $>10a_0$ in Lu:1221 at 600 Oe, the maximum field studied. We speculate that the anomalous maximum seen here, at which point we also observe strong departure from the collective pinning model, arises from the shear properties of the FLL. The finite critical current throughout this regime further suggests that the high field disordering is a static effect, rather than a dynamic disordering such as melting.

In Fig. 2, we also show data for the field rotated by 30° from the c axis, where the FLL has distorted hexagonal symmetry. In this orientation we also find that ξ_L is dominated by the shear strength, although the low field ξ_L is considerably reduced in this case.

Within the 3D collective pinning model, the longitudinal Larkin-Ovchinnikov length can be expressed as $L_c = 2c_{66}c_{44}\xi^2(1/nf^2)$ where c_{44} is the tilt modulus, c_{66} is the shear modulus, and nf^2 is the elemental pinning force [13]. As pointed out by Giamarchi and Le Doussal [21], L_c in this theory differs from ξ_L measured in a SANS experiment by constant times $(a_0/\xi)^2$. This leads to $\xi_L \sim 2c_{66}c_{44}a_0^2(1/nf^2)$. In the same model, the elemental pinning force is related to the critical current via $J_cB/c = n^2f^4/2c_{44}c_{66}^2\xi^3$, leading to $\xi_L/a_0 = A(2c_{44}ca_0^2/\xi^3J_cB)^{1/2}$, with A being a constant. Note that only the tilt modulus enters into this equation. Shown in Fig. 3 are the results from critical current measurements in Lu:1221 with $\mathbf{H} \parallel \mathbf{c}$. Voltage criteria between 0.1 and 0.35 μV/cm were used to determine the onset of flux flow resistivity. Plotted is the pinning force density J_cB as a function of field. The data show a large peak effect near 60 kOe [$H_{c2}(T = 2.2\text{ K}) = 65$ kOe] and a weak maximum near 10 kOe. Also shown in the figure is L_c/a_0 ignoring dispersion in $c_{44} = BH/4\pi$. The solid line is a simple expression valid when J_cB is constant. The value of ξ_L with the constant $A = 1/70$ is plotted in Fig. 2 as the solid line for comparison with the SANS data.

Clearly, the structural and transport data agree within the framework of the collective pinning model for fields below the 10 kOe, but sharply disagree for fields greater than this. We have similar qualitative results for Y:1221. Even the weak maximum in J_cB at 10 kOe would produce a local minimum in ξ_L, rather than the observed maximum. In previous studies of Nb and $NbSe_2$ this collective pinning analysis works well up to the peak effect in relating J_cB and ξ_L [18,19]. We believe that the breakdown of this analysis and the observed high field disordering is related to the anomalous shear properties of the FLL in this system. The square to hexagonal transition at low fields further suggests that the shear modulus of the square lattice is unusually small. For an hexagonal FLL (we do not have expressions valid for the square FLL), the shear modulus can be approximated by $c_{66} \propto (H_c^2/16\pi)b(1 - 0.29b)(1 - b)^2$ where $b = B/B_{c2}$ [22]. This expression has a peak near $b \sim 0.3$, and provides an excellent overall fit to our data, although the fitted values of H_{c2} tend to be about 15% low.

There are two routes which may lead to the shear modulus c_{66} controlling the behavior of ξ_L. First, since the square FLL is stabilized by nonlocal corrections to the London model, the statistical summations which lead to the cancellation of c_{66} in the expressions for the longitudinal correlation length may need to be modified. Second, the assumption of isotropic continuum elasticity may be too gross an oversimplification. Clearly, the shear properties are quite anisotropic at the square-hexagonal FLL transition, at which the shear strength was found to vanish only in one particular direction in numerical studies [23].

In conclusion, we have used SANS and transport to study the FLL in Lu:1221 and Y:1221. In both cases, the low field, hexagonal FLL transforms into a square FLL for fields greater than $\sim$1 kOe. We see a significant, static disordering in the square lattice phase at $H/H_{c2} \sim 0.2$, at which point the simple collective pinning model breaks down. We attribute this disordering to the anomalous shear properties of the square FLL, although there is clearly a need for more theoretical understanding of the correlation lengths in this case. It is interesting to compare these data to our studies in Er:1221 [9,11]. In that case, the low field data also followed the collective pinning model. However, the data departed abruptly at 1.5 kOe, above which ξ_L was field independent. In that case we believe the abrupt departure is related to strong pinning to magnetic domain walls in the antiferromagnetic superconducting phase, which has also not been considered in collective pinning models.

This work was supported by NATO under Grant No. CRG960550. M. R. E. is supported by the Danish Research Academy. P. C. C. is supported by the Director of Energy Research, Office of Basic Energy Science under Contract No. W-7405-Eng.-82. We thank V. Kogan, R. Cava, and B. Batlogg for valuable discussions.

[1] T. Siegrist *et al.*, Nature (London) **367**, 254 (1994).
[2] R. Nagarajan *et al.*, Phys. Rev. Lett. **72**, 274 (1994).
[3] R. J. Cava *et al.*, Nature (London) **367**, 252 (1994).
[4] M. Xu *et al.*, Physica (Amsterdam) **227C**, 321 (1994); H. Takagi *et al.*, Physica (Amsterdam) **228C**, 389 (1994).
[5] B. K. Cho *et al.*, Phys. Rev. B **52**, 3684 (1995).
[6] C. V. Tomy, G. Balakrishnan, and D. McK. Paul, Physica (Amsterdam) **248C**, 349 (1995).
[7] T. K. Ng and C. Varma, Phys. Rev. Lett. **78**, 330 (1997); K. D. D. Rathnayaka *et al.*, Phys. Rev. B **53**, 5688 (1996).
[8] R. J. Cava *et al.*, Physica (Amsterdam) **235-240C**, 154 (1994).
[9] U. Yaron *et al.*, Nature (London) **382**, 236 (1996).
[10] Y. De Wilde *et al.* (to be published).
[11] M. R. Eskildsen *et al.*, Phys. Rev. Lett. **78**, 1968 (1997).
[12] V. G. Kogan *et al.*, Phys. Rev. B **55**, R8693 (1997); I. Affleck *et al.*, Phys. Rev. B **55**, R704 (1997).
[13] A. I. Larkin and Yu. N. Ovchinnokov, J. Low Temp. Phys. **34**, 409 (1971); M. Tinkham, *Introduction to Superconductivity* (McGraw-Hill, New York, 1996).
[14] J. Schelten, G. Lippmann, and H. Ullmaier, J. Low Temp. Phys. **14**, 213 (1974); G. Lippmann, J. Schelten, and W. Schmatz, Philos. Mag. **33**, 457 (1976).
[15] M. O. Mun *et al.*, Phys. Rev. Lett. **76**, 2790 (1996).
[16] H. Pastoriza and P. H. Kes, Phys. Rev. Lett. **75**, 3525 (1995); M. H. Theunissen, E. Van der Drift, and P. H. Kes, *ibid.* **77**, 159 (1996); Hui Wu *et al.*, *ibid.* **78**, 334 (1997).
[17] P. L. Gammel *et al.*, Phys. Rev. Lett. **72**, 278 (1994).
[18] U. Yaron *et al.*, Phys. Rev. Lett. **73**, 2748 (1994); **74**, 1700(E) (1995); U. Yaron *et al.*, Nature (London) **376**, 753 (1995).
[19] P. L. Gammel *et al.*, Proc. International Symposium on Advances in Superconductivity: New Materials, Critical Currents and Devices, Sept. 17–20, 1996, Mumbai, India (to be published).
[20] G. Blatter *et al.*, Rev. Mod. Phys. **66**, 1125 (1994).
[21] T. Giamarchi and P. Le Doussal, Phys. Rev. Lett. **75**, 3372 (1995); U. Yaron *et al.*, *ibid* **75**, 3373 (1995).
[22] E. H. Brandt, Phys. Status Solidi B **77**, 551 (1976); P. H. Kes and C. C. Tsuei, Phys. Rev. B **28**, 5126 (1983).
[23] V. G. Kogan (private communication).